Second order effects in the algebraic potential for heavy-ion systems near the Coulomb barrier

R. Lichtenthäler, D. Pereira, L. C. Chamon, and L. C. Gomes
Instituto de Física da Universidade de São Paulo, Laboratório Pelletron, C. P. 20516, CEP 01452-990, São Paulo, S. P., Brazil

A. Ventura
Ente Nuove Tecnologie, Energia e Ambiente, Viale Ercolani 8, I-40138, Bologna, Italy

L. Zuffi
Dipartimento Di Fisica dell'Università di Milano, Italy, and Istituto Nazionale di Fisica Nucleare, Sezione di Milano, Via Celoria 16, I-20133 Milano, Italy
(Received 26 July 1994)

The energy dependence of the algebraic potential for heavy-ion elastic scattering near to the Coulomb barrier is investigated. The inclusion of an additional term in the complex algebraic potential to take into account the reflection due to the imaginary well is proposed. With this new term 12 elastic scattering angular distributions of the $^{16}O+^{63}Cu$ system ranging from $E = 39$ to 64 MeV in the laboratory system were analyzed. The real and imaginary strengths of the algebraic potential exhibit a dependence with energy similar to the dispersive behavior associated with the threshold anomaly.

PACS number(s): 25.70.Bc, 24.10.−i

I. INTRODUCTION

The algebraic scattering theory (AST) proposed by Alhassid and Iachello [1] is a useful method for analyzing heavy-ion scattering data. One of the most practical versions of AST is based on SO(3,1) symmetry. In this case the S matrix can be written as a ratio of two Euler gamma functions:

$$S_\ell = \frac{\Gamma(\ell + 1 + iv)}{\Gamma(\ell + 1 - iv)}, \tag{1}$$

where v, called the algebraic potential, is equal to the Sommerfeld parameter $\eta = \mu Z_1 Z_2 e^2/\hbar^2 k$ for the case of a pure Coulomb interaction. In this case the symmetry is exact. In order to take into account the strong interaction, the algebraic potential must be generalized to be dependent on the angular momentum ℓ:

$$v(\ell) = \eta + v_s(\ell). \tag{2}$$

Absorption can be taken into account by making the algebraic potential complex provided $\mathrm{Im}(v) \geq 0$ to guarantee unitary bound for the S matrix. A few models have been proposed for the ℓ dependence of the real and imaginary parts of the algebraic potential [1,2]. Also theoretical investigations based on semiclassical methods have given some insight into the shape of the algebraic potential for high values of ℓ [3,4]. In general, these models are based on a Woods-Saxon shape in ℓ space similar to the Woods-Saxon well commonly used in the usual optical model calculations. By means of an inversion procedure developed by two of us [2] we were able to investigate the behavior of $v(\ell)$ that exactly reproduces the S matrix obtained from realistic optical model calculations. This study shows that second order contributions of the imaginary part to the real potential are very important and should be included in the algebraic potential in order to give a more precise description of the scattering between heavy ions.

II. EXPERIMENTAL DETAILS

The elastic scattering cross sections for the $^{16}O+^{63}Cu$ system have been measured using the ^{16}O beam from the 8UD Pelletron Accelerator. The detecting system was a set of nine surface barrier detectors spaced 5° apart. The solid angle between each detector and the target was 10^{-4} sr with an angular aperture $\Delta\theta = 0.5°$. The typical thickness of the enriched (99.9%) Cu target was 30 μg/cm^2 evaporated onto a 5 μg/cm^2 carbon foil, for the low energy measurements 39 MeV $\leq E_{\mathrm{lab}} \leq$ 46 MeV and self-supporting targets with thickness between 60 and 80 μg/cm^2 for the high energy measurements 47 MeV $\leq E_{\mathrm{lab}} \leq$ 64 MeV. In both cases, a thin layer of gold was evaporated onto the targets for data normalization, and we have used a surface barrier detector as a monitor, to be sure of no target deteriorations during the measurements. The energy resolution was 200 keV, which allows a good separation between the elastic peak and the inelastic group corresponding to the excitation of the first five low lying states of the ^{63}Cu nucleus. Figure 1 exhibits as dots the experimental data for the measured 12 angular distributions in the ranges 39 MeV $\leq E_{\mathrm{lab}} \leq$ 64 MeV and 40° $\leq \theta_{\mathrm{c.m.}} \leq$ 175°.

0556-2813/94/50(6)/3033(4)/$06.00

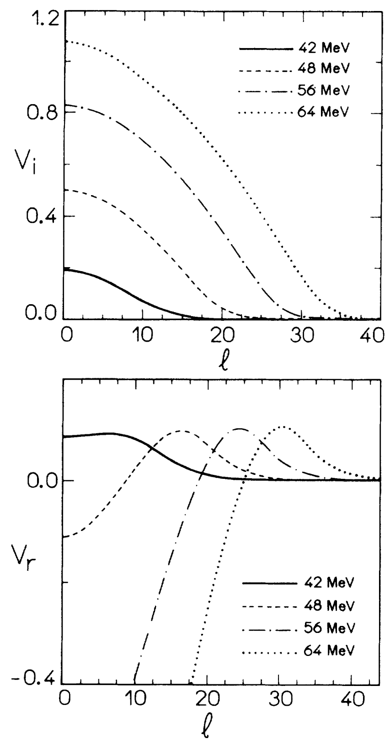

FIG. 1. In the upper part we exhibit the imaginary part of the algebraic potential obtained by inversion of optical model S matrix at the energies 42, 48, 56, and 64 MeV. In the bottom the same for the real part of the algebraic potential.

III. RELATION BETWEEN OPTICAL MODEL AND ALGEBRAIC POTENTIAL

One of the most interesting aspects of the SO(3,1) S matrix [Eq. (1)] is the simplicity of the inverse problem $S(\ell)$ to $v(\ell)$. It can be easily solved by expanding the S matrix in a Taylor series [2] around v^0 and taking the first term of the expansion, and we have

$$v(\ell) = v^0 + \frac{-i\ln(S/S^0)}{\psi(\ell+1+i\eta+iv^0)+\psi(\ell+1-i\eta-iv^0)},$$

where ψ is the digamma function. For high partial waves ($\ell \geq 2\ell_g$) we have $v^0 \approx 0$ and

$$S^0 = \frac{\Gamma(\ell+1+i\eta)}{\Gamma(\ell+1-i\eta)}.$$

For large values of the Sommerfeld parameter we can use the asymptotic form for the digamma function $\psi \rightarrow \ln$ and one obtains

$$v(\ell) = \frac{\delta_r + i\delta_i}{\ln[(\ell+1)^2+\eta^2]^{1/2}}. \tag{3}$$

Equation (3) shows that the real and imaginary parts of the algebraic potential are related to the phase shift $\delta_r + i\delta_i$ in a straightforward way. In many situations involving heavy-ion scattering, Eq. (3) is sufficiently accurate but, for exact numerical results, Eq. (2) has to be solved iteratively. We applied Eq. (2) to determine the algebraic potential corresponding to a Woods-Saxon optical potential in the Schrödinger equation that reproduces the elastic scattering angular distributions of the $^{16}O+^{63}Cu$ system for laboratory energies from 39 to 64 MeV. The parameters of this optical potential were assumed to be constant in the whole energy range. In Fig. 1 we present the real and imaginary parts of the algebraic potential obtained by inversion at the energies 42, 46, 56, and 64 MeV. We observe that in spite of the fact that the optical potential is constant with energy, the same does not happen in the algebraic one. As the imaginary part increases, the real potential bends down to negative values in the region $\ell \leq \ell_g$. This is an indication that there is a repulsive term in the potential which causes the nuclear deflection function $2d\delta_r/d\ell$ to be positive in this region. The decreasing of the real algebraic potential with energy for low values of ℓ confirms the presence of a repulsive potential. For higher values of the angular momentum $\ell \geq \ell_g$ the algebraic potential becomes positive, again decreasing exponentially with ℓ as expected for an attractive nuclear potential [3]. This repulsive term has a simple optical interpretation. It corresponds to a reflection in the imaginary well that manifests with a real phase shift and therefore a real algebraic potential. In order to parametrize this term we suggest the following form:

$$v_s(\ell) = v_s^0(\ell) + \alpha(v_s^0(\ell))^2 \quad \text{for} \ \mid v_s^0 \mid < 1,$$

with

$$v_s^0(\ell) = v_r f_r(\ell) + i v_i f_i(\ell),$$

where v_r and v_i are the strengths and $f_r(\ell)$ and $f_i(\ell)$ the Woods-Saxon form factors of the real and imaginary algebraic potentials, respectively. With these considerations we have

$$v_s(\ell) = v_r f_r(\ell) - \alpha v_i^2 f_i(\ell)^2 + i v_i f_i[1 + 2\alpha v_r f_r(\ell)].$$

In our analysis we simplified somewhat the above equation. First we arbitrarily assumed $\alpha = 1$, to reduce the number of parameters involved. We neglected the positive term that modulates $v_i f_i(\ell)$ on the assumption that its effects are to a large extent taken under consideration in the choice of the parameters for $\mathrm{Im}(v_s)$. The second term we took explicitly into account as, being negative, it cannot be simulated by any reasonable variation of the parameters for $\mathrm{Re}(v_s)$. Therefore we set

$$v_s(\ell) = v_r f_r(\ell) - v_i^2 f_i^2(\ell) + i v_i f_i(\ell). \tag{4}$$

Equation (4) has six parameters which are the two strengths, the two grazing angular momenta, and the two diffuseness for the real and imaginary parts. With these parameters one reproduces very well the shapes of Fig. 1. It is interesting to note that even if the real strength v_r is zero, we still have a contribution to the real part of the algebraic potential that comes from the second term in Eq. (4). We have also observed this fact in optical model

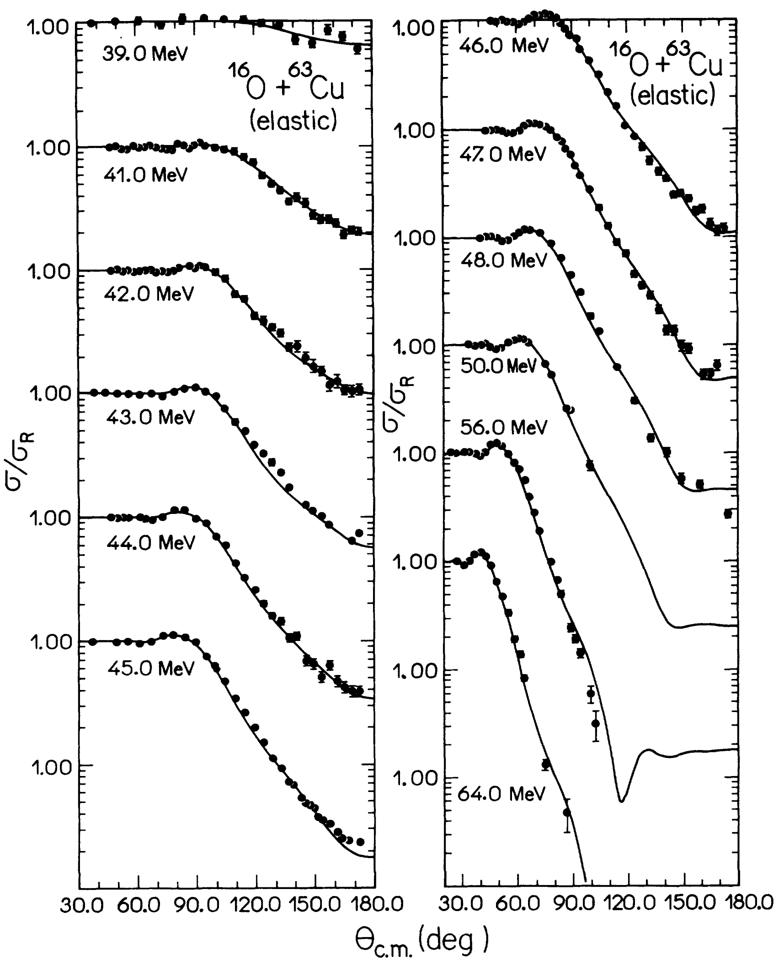

FIG. 2. The elastic angular distributions for the 12 energies measured. The solid curve is the result of our calculations.

calculations when even with a zero real potential there still remains a negative real phase shift which comes from the reflection in the imaginary well.

IV. ANALYSIS AND RESULTS

Using Eq. (4) we analyzed the 12 elastic angular distributions at energies ranging from $E_{\rm lab}$ = 39 up to 64 MeV, the Coulomb barrier being at $E_{\rm lab}$ = 40 MeV. The six parameters have been freely varied to reproduce the experimental data. In Fig. 2 we show our results. The reduced chi square of the fits is about unity or even lower at some energies. In Fig. 3 we plot the strengths of the real and imaginary potentials obtained as a function of the energy. The solid curve in Fig. 3 is only a guide to the eyes. An interesting phenomenon occurs at the energies around 43 MeV where the strength of the real potential presents a maximum. This behavior is necessary to reproduce the principal maximum of the diffraction of the data at forward angles. If we do not increase the real potential at these energies, the calculated angular distributions become flat in this region, in disagreement with the experimental data which still present maxima for 42,

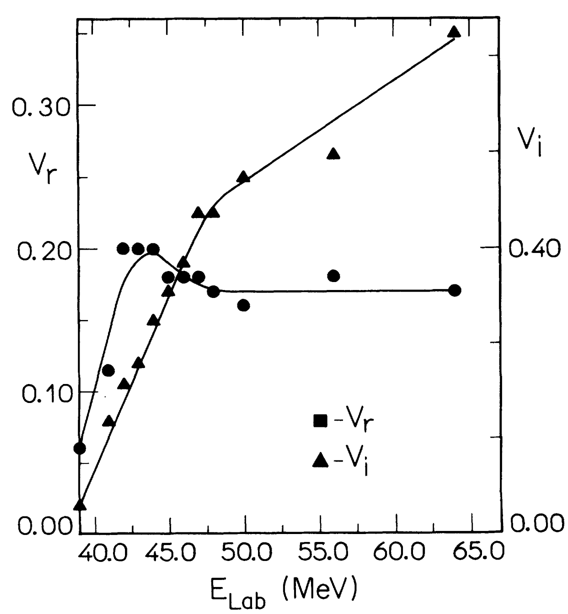

FIG. 3. The values of the strengths v_r and v_i of the real and imaginary parts of the algebraic potential as a function of the energy.

43, and 44 MeV. For lower energies the real potential goes to zero since we are below the Coulomb barrier. Above 46 MeV the real potential seems to become constant. The imaginary strength increases with energy although apparently in a less pronounced way for higher energies. This is expected due to the opening of reaction channels mainly coming from the inelastic excitations. As can be seen in Fig. 3, the real strength v_r of $v_s(\ell)$ exhibits in the neighborhood of the Coulomb barrier a variation with energy similar to the one associated with the threshold anomaly observed in the optical potential analysis using the Schrödinger equation [5]. We believe that this anomalous behavior is observed in the algebraic potential because second order effects were taken into consideration, leaving the real strength v_r in Eq. (4) directly related to the real strength of the optical potentials used in the Schrödinger equation. This point is at the moment subject to further investigation.

The form factor grazing angular momenta, used in the algebraic potential, follow approximately the relation $\ell_g = kR$ where $k = \sqrt{2\mu(E - E_b)}/\hbar$ and E_b is the Coulomb barrier. If we adjust R and E_b to reproduce the values of the imaginary grazing angular momentum, we obtain $E_b = 32.2$ MeV and $R = 7.6$ fm, which agree with the values obtained from fusion measurements and optical model calculations for this system [6].

V. CONCLUSIONS

We analyzed the elastic scattering angular distributions for the $^{16}O+^{63}Cu$ system at several energies from the neighborhood of the Coulomb barrier $E_{\rm lab} = 39$ up to 64 MeV in the context of the algebraic scattering theory. An inversion procedure allowed us to investigate the relation between the optical model S matrix and the algebraic potential and revealed that second order effects like reflection in the imaginary well are very important to give a realistic description of the scattering between heavy ions. We propose a simple way to parametrize this effect which seems to work very successfully for this system. The fits obtained are of very good quality and allow us to observe the behavior of the algebraic potential at energies near the Coulomb barrier.

[1] Y. Alhassid and F. Iachello, Nucl. Phys. **A501**, 585 (1989).
[2] R. Lichtenthaler Filho, A. C. C. Villari, L. C. Gomes, and P. Carrilho Soares, Phys. Lett. B **269**, 49 (1991).
[3] M. S. Hussein, M. P. Pato, and F. Iachello, Phys. Rev. C **38**, 1072 (1988).
[4] K. Amos, L. Berge, L. J. Allen, and H. Fiedeldey, Phys. Rev. C **47**, 2827 (1993).
[5] G. R. Satchler, Phys. Rep. **199**, 147 (1991).
[6] L. C. Chamon, D. Pereira, E. S. Rossi, C. P. Silva, G. R. Razeto, A. M. Borges, L. C. Gomes, and O. Sala, Phys. Lett. B **275**, 29 (1992).